Green Chemistry

COMMUNICATION

View Article Online
View Journal

Cite this: DOI: 10.1039/c8gc03039a

Received 27th September 2018,
Accepted 7th December 2018

DOI: 10.1039/c8gc03039a

rsc.li/greenchem

Automated and accelerated synthesis of indole derivatives on a nano-scale†

Shabnam Shaabani, ‡[a] Ruixue Xu,‡[a] Maryam Ahmadianmoghaddam,[a] Li Gao,[a] Martin Stahorsky,[a] Joe Olechno,[b] Richard Ellson,[b] Michael Kossenjans,[c] Victoria Helan[c] and Alexander Dömling *[a]

Automated, miniaturized and accelerated synthesis for efficient property optimization is a formidable challenge in chemistry in the 21st century as it helps to reduce resources and waste and can deliver products in shorter time frames. Here, we used for the first time acoustic droplet ejection (ADE) technology and fast quality control to screen the efficiency of synthetic reactions on a nanomole scale in an automated and miniaturized fashion. The interrupted Fischer indole combined with Ugi-type reactions yielded several attractive drug-like scaffolds. In 384-well plates, a diverse set of interrupted Fischer indole intermediates were produced and reacted with the tricyclic hydantoin backbone in a 2-step sequence. Similarly, preformed Fischer indole intermediates were used to produce diverse sets of Ugi products and the efficiency was compared with that of the *in situ* method. Multiple reactions were performed again on a preparative millimole scale, showing scalability from nano to mg and thus synthetic utility. An unprecedented large number of building blocks were used for fast scope and limitation studies (68 isocyanides, 72 carboxylic acids). Miniaturization and analysis of the generated big synthesis data enabled deeper exploration of the chemical space and permitted the gain of knowledge that was previously impractical or impossible, such as the rapid survey of reactions, and building block and functional group compatibility.

Automation is a global force that will transform economies and the workforce[1]

In the age of artificial intelligence, miniaturization, automation and acceleration of experimental data collection is a prerequisite in modern science and technology, and is already well established in many areas of molecular and cell biology, medicine, materials science, engineering and physics.[2–4] Organic synthesis of new matter is a central science and technology and it contributes in societal progress through novel medication, efficient and safe plant protection, new materials, contributors to human health, food supply.[5–8] Nonetheless, small molecule synthesis laboratory technology mostly is at a stage not much different from what it was 200 years ago. Reactions are performed sequentially often unnecessarily on a large scale by synthesizing small arrays of compounds and are not targeted towards the goal of discovery of novel properties (Fig. 1). While major progress has been made in new catalysis, novel reactions, and stereoselective synthesis, the pace of synthetic reactions is slow with typically ~1–5 reactions per worker/FTE per week.[8]

Although there exist very useful automated methods for the assembly of specialized molecule classes such as peptides, oligonucleotides, and oligosaccharides, their synthetic scope is rather limited. Only a few and similar molecular building blocks and less than half a dozen reactions are used.[9,10] Attempts to automate the synthesis of certain natural products using a few reliable coupling reactions and rather easily accessible building blocks are also described.[9] Automated synthesis therefore recently became an important topic in synthetic engineering.[11] Key to miniaturization and acceleration of synthetic chemistry are reactors of small dimensions and fast, precise and efficient building block dispensing methods. While pico-, femto- and attoliter reactor sizes have been described, implementation of this scale of synthesis in a flexible and high-throughput manner has been largely unexplored.[12–14]

Nano one-pot reactions

Here, we use ADE-enabled fast, automated and nanomole scale organic synthesis exemplified by scouting the reaction spaces of the interrupted Fischer indole and different Ugi

[a]University of Groningen, Department of Drug Design, A. Deusinglaan 1, 9713 AV Groningen, The Netherlands. E-mail: a.s.s.domling@rug.nl
[b]Labcyte Inc., 170 Rose Orchard Way, San Jose, CA 95134, USA
[c]Hit Discovery, Discovery Sciences, IMED Biotech Unit, AstraZeneca, Gothenburg, SE-43183 Mölndal, Sweden

†Electronic supplementary information (ESI) available. See DOI: 10.1039/c8gc03039a

‡These authors contributed equally to this work.

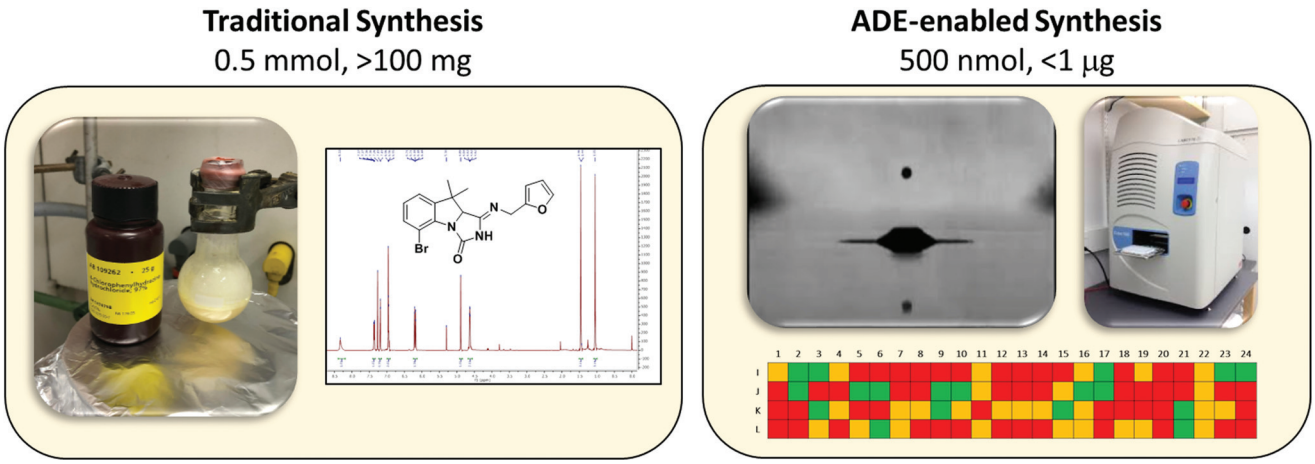

Fig. 1 Traditional and ADE-enabled synthetic chemistry. ADE-enabled synthetic chemistry needs a fraction of the materials compared to traditional chemistry. Many more building block combinations can be evaluated and rich datasets are produced which would be too time-consuming and expensive to generate traditionally.

multicomponent reaction modifications. ADE technology uses sound waves applied to liquids to generate and precisely transport nanoliter droplets.[15] Isocyanide-based multicomponent reactions (IMCRs) are a highly relevant reaction class and span a relevant chemical space in drug discovery as they enable easy discovery and/or access to multiple commercial and experimental drugs, *e.g.* anti-pain carfentanil and xylocaine,[16,17] anti-seizure lacosamide,[18] anti-depressant olanzepine,[19] blood coagulant rivaroxaban and clopidogrel,[20,21] HCV drug telaprevir,[22] birth-controlling epelsiban,[23] or cancer-starvation ivosidenib,[24] just to mention a few. In particular, IMCR is robust, scalable, safe, and green and fulfils the important requirement of tolerating nitrogen heteroatoms and (unprotected) polar functional groups common in drug molecules for syntheses.[25–27] Thus, novel modifications of IMCR scaffolds are an intensive area of research and innovation.[28] Schiff bases are key intermediates in the majority of the very versatile IMCRs. Cyclic Schiff bases **3** of high diversity can be formed by an interrupted Fischer indole synthesis, whereby α,α′-disubstituted carbaldehydes react under acidic conditions with (hetero)aromatic hydrazines.[29,30] *Per se* this is a highly versatile synthetic transformation, since many aldehyde and hydrazine building blocks can be potentially combined resulting in a large number of low molecular weight key intermediates for further derivatizations in an overall short sequence of steps.[31] To better understand the scope and limitations of the combination of different building blocks, we planned to investigate the interrupted Fischer indole reaction in combination with several IMCRs **4–6** (Scheme 1).

The three reactions we combined with the interrupted Fischer reaction **3** were the Ugi three-component reaction (U-3CR) **4**, the Ugi tetrazole reaction (UT-3CR) **5** and the Ugi imino hydantoin reaction (UH-3CR) **6**. First, we synthesized and isolated a number of interrupted Fischer building blocks on a gram scale (Scheme 1, Fig. 2).[29,30]

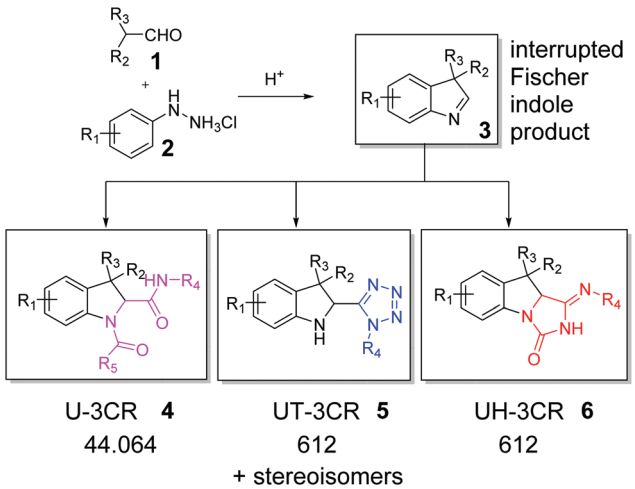

Scheme 1 Investigated interrupted Fischer indole/IMCR scaffolds and theoretically accessible chemical space based on the used building blocks.

Next, we synthesized 192 random combinations of 9 cyclic Schiff base building blocks with 68 different isocyanides and 72 carboxylic acids to yield 48 imino hydantoin and 48 tetrazole and 96 U-3CR products, respectively (Fig. 2). The reagents were dissolved in ethylene glycol or 2-methoxyethanol (carboxylic acids) as 0.5 M stock solutions and kept in a 384-well source plate and transferred into a corresponding 384-well destination plate using an Echo555 acoustic dispenser. The solvent ethylene glycol was chosen because of its similarity to the often-used methanol for IMCRs and to account for a viscous not volatile transport solvent required in ADE. The scale of each discrete reaction per well was 375 or 500 nanomole, for UH-3CR and U-3CR and UT-3CR, respectively. 750 or 1000 nL of each building block was transferred into the destination plate which was accomplished in less than 1.5 h (ESI†).

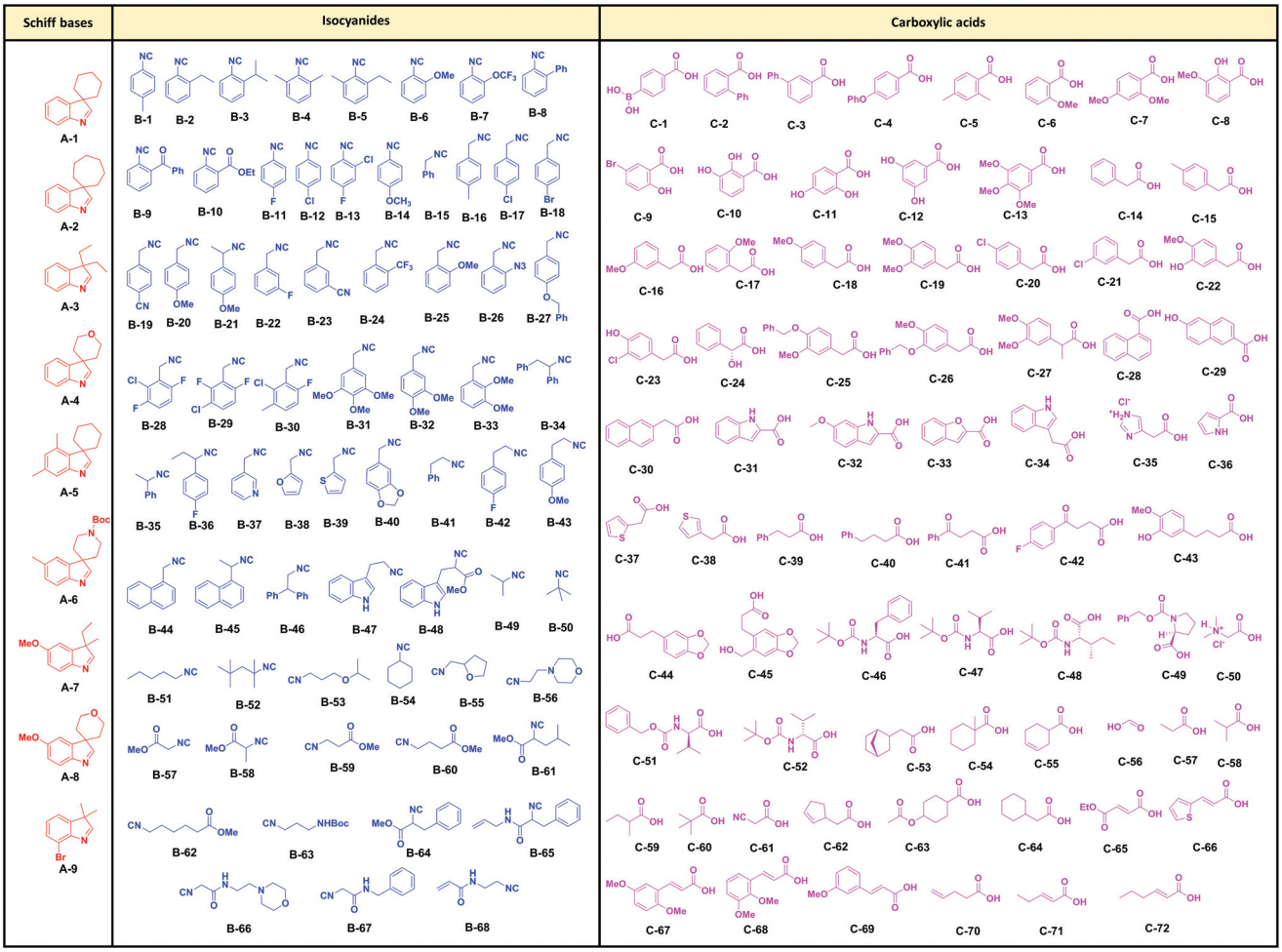

Fig. 2 Diversity of cyclic Schiff base, isocyanide, carboxylic acid and other building blocks used.

The plate was left sealed for 12 h to react at room temperature. Then, the reactions were analyzed overnight using automatic SFC-MS and TLC-MS (Fig. 3, ESI†). The analysis revealed that a total of 159 products (designated with green and yellow colors: 83%) out of 192 reactions were formed and 114 products were in good quantities (green). Amongst the three investigated reactions, the imino hydantoin synthesis (UH-3CR) worked best with 92% of the wells showing product formation, followed by U-3CR (81%) and tetrazole synthesis (77%) (ESI†).

Noteworthily, multiple polar building blocks in all functional group classes worked well, including morpholine (**B68**), pyridine (**B37**), tetrahydrofuran (**B55**), tetrahydropyran (**A8**) and unprotected boronic acid (**C1**). This is important to keep control over the lipophilicity of the final products. Subtle reactivity trends were discovered in the data analysis which traditionally would be much more cumbersome to obtain. For instance, it was found that phenyl unsubstituted indoles (**A1–A4**) were more reactive (ESI†). This trend was visible for all three Ugi-type reactions (**4**, **5**, and **6**). Amongst the phenyl substituted indoles, the 5-Br substrate **A9** surprisingly represented an island of reactivity with 66% success rate in all reactions.

The information density produced by ADE-enabled nanoscale synthesis permits reactivity explorations that were previously impractical or impossible, such as the rapid survey of building blocks and several scaffolds at once. Patterns of the functional group compatibility of the carboxylic acids in U-3CR **4** include free boronic acid (**C1**), biphenyls (**C2**, **C3**); free phenolic –OH in different positions (**C8**, **C9**, **C11**, **C12**, **C29**, **C43**); several heterocyclic carboxylic acids including indole (**C31**, **C32**, **C34**), benzofurane (**C33**), pyrrole (**C36**), thiophene (**C38**), thiophene cinnamic acid (**C66**) worked well; several chiral *N*-protected amino acids (**C47**, **C48**, **C49**, **C52**) yielded the expected products and aliphatic hydroxy groups were compatible in **C45**. Bulky and small aliphatic groups were well tolerated; alkenes in different positions (**C66**, **C67**, **C68**, **C70**, **C71**) and nitrile (**C61**) are also compatible; however, *meta* substituted cinnamic acid (**C69**) did not give any product. Overall, scaffold **4** showed a very good tolerance to protected and unprotected carboxylic acid groups. A great functional group compatibility is the signature of a synthetically valuable reaction. Similar findings could be observed in the other scaffolds, **3** and **5**.

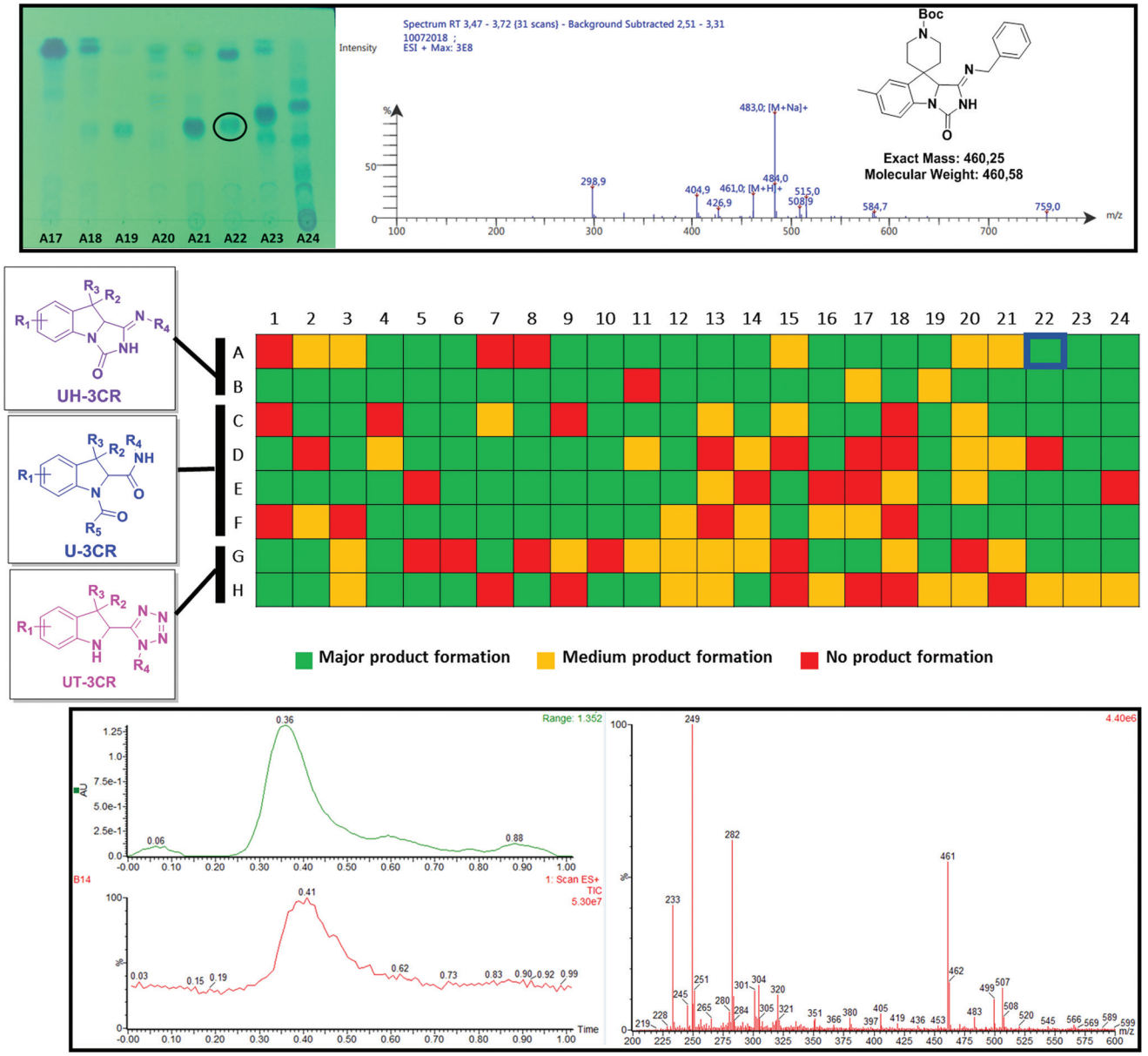

Fig. 3 Heat plot of the 192-well array of interrupted Fischer/MCR chemistries based on SFC-MS analysis and exemplary TLC-UV-MS (above) and SFC-MS (below) analyses of well **A22**.

The diversity of isocyanides used in this HT experiment is unprecedented. An unprecedented high number of 68 highly diverse isocyanides were brought to reaction, ranging from aromatic to aliphatic to bulky to linear aliphatic to heterocyclic ones (morpholine, furan, tetrahydrofuran, indole, pyridine). Functional group compatibility was tested positive for example with amides (**B65–B67**), acrylamides (**B68**), ethers (**B53**, **B55**), and esters (**B48**, **B57**, **B58**, **B60**, **B62**). Among the esters, ethyl 2-isocyanobenzoate (**B10**) did not give any product.

Synthetically useful methods should be scalable to ensure rapid adaption by industry to utilize novel synthetic transformations. To show smooth scalability, we resynthesized and fully characterized 23 unprecedented representative molecules of the 192-nanoscale reactions on a 1 mmol scale (ESI†): 10 imino hydantoins **6**, 7 U-3CR **4** and 6 tetrazoles **5** (Fig. 4). The isolated yields varied between 26 and 96% with an average of 60%.

Finally, we investigated the possibility of forming the interrupted Fischer indole products *in situ* on a nmol-scale and subsequently adding the reagents for the UH-3CR scaffolds, in order to avoid the time-consuming traditional synthesis of the key cyclic Schiff bases. A random array of 96 reactions was performed based on 9 aromatic hydrazine hydrochlorides and 9-α,α-disubstituted aldehydes which were first reacted, followed by addition of aqueous potassium cyanate, Py·HCl and isocyanides. It was found that the *in situ* reaction performed worse

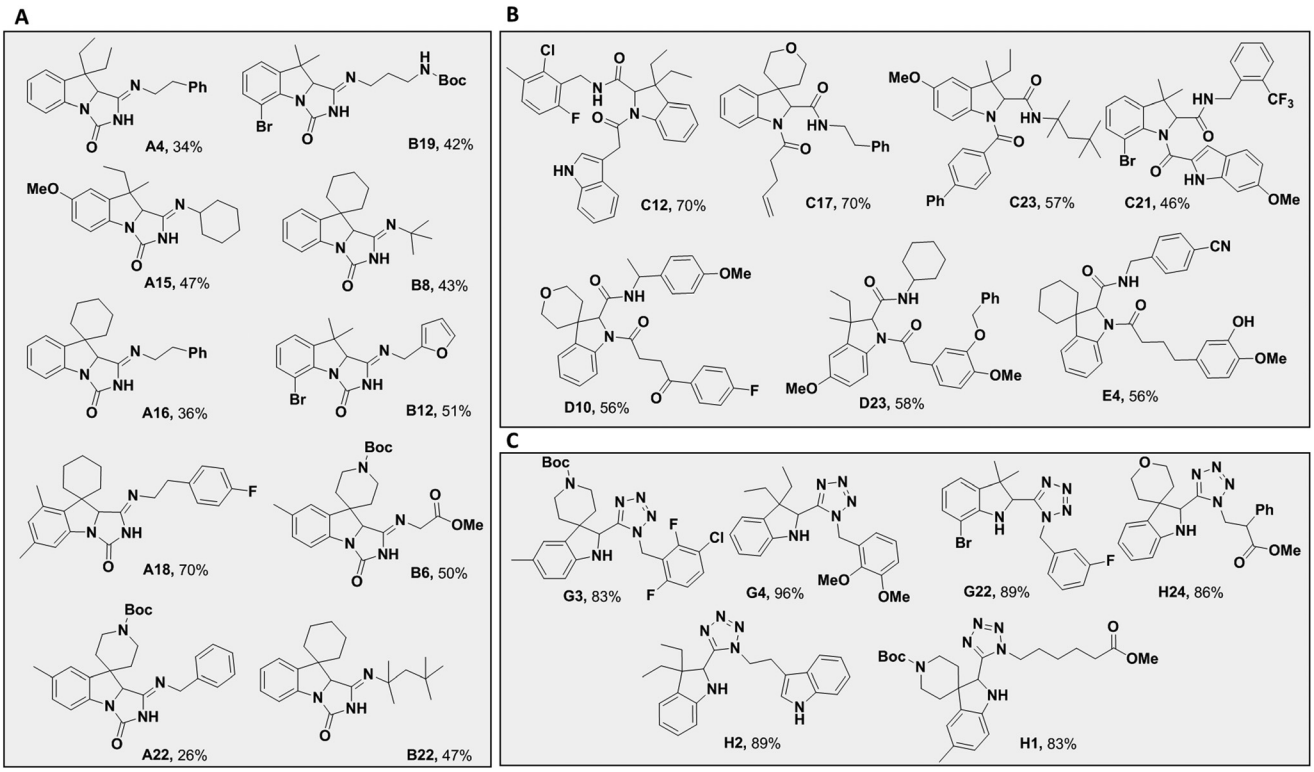

Fig. 4 Resynthesized compounds based on the three scaffolds **4–6** and on their performance in the nano-synthesis (Fig. 3).

(48%) than the stepwise procedure (92%) using dispensed purified interrupted Fischer indoles (Fig. 5). Still, the much greater variability of accessible cyclic Schiff bases points to the possibility of synthesizing a very large chemical space of tricyclic hydantoins with 3 highly variable building blocks (arylhydrazines, aldehydes, and isocyanides).

ADE is a technology which has already found application in medicine, genetics, biotechnology, high throughput screening and protein crystallography.[32] Surprisingly, however, no applications in the area of miniaturization and acceleration of the synthesis of small molecules have been published. ADE-enabled synthesis introduced here has several distinct advantages over classical tip-based dispensing. It is a precise, accurate and contactless dispensing technology suitable for rapid transport of nanolitre amounts of reagent stock solutions from a source to a destination plate.[15] With a frequency of >100 hertz 2.5 nanolitre-sized droplets can be transported into nano-reactors to perform thousands of discrete reactions in only a few hours. The 'touch-less' feature comes with a 'consumable-less' feature as compared to other tip-based nano-dispensing systems.[33] Moreover, it avoids potential sources of impurities by leakage of plastic additives. Combined ADE-enabled synthesis and fast quality control using TLC-MS and SFC-MS was used here to scout three different reactions and enable the mmol resynthesis of 23 unprecedented exemplary compounds in good-to-excellent yields. Recently introduced 384- and 1536-well high density and sealable glass plates or classical polypropylene plates promise to enable a wide variety of classical and new synthetic organic reactions including transition-metal catalysis by ADE (Fig. 6).[34]

High throughput experimentation methods empower chemists to run orders of magnitude more experiments and enable "big data" informatics approaches to reaction design and troubleshooting.[26,35–37] The herein introduced nanoscale and high throughput ADE-enabled platform provides unprecedented insight into structure–reactivity relationships (SRR). In traditional reaction discovery/screening, optimization is done under a few conditions leading to the mmol-scale synthesis with a low-density array of novel compounds. 'Real-world' scope and limitation studies including drug-like hydrophilic fragments to test the level of tolerance of a reaction toward the polar functional groups and nitrogen heteroatoms found in biologically active molecules are impossible to be performed with reasonable resources, costs and in time using a traditional mmol-based approach. Another advantage is the minute reagent consumption. The ADE-enabled chemistry at the nanoscale led to a total reagent consumption to scout 288 reactions of less than 4 mg. For comparison, in a traditional 1 mmol scale per reaction, 150 g of starting material would be used in addition to 75 L of solvent just to perform the reactions. Consequently, precious starting materials, such as a large number of complex isocyanides, can be used here. Moreover, due to the high degree of automation of the ADE-platform, chemists have less contact with potentially hazardous chemicals, solvent fumes and reactions, contributing critically to safety aspects. On the other hand, it should be noted

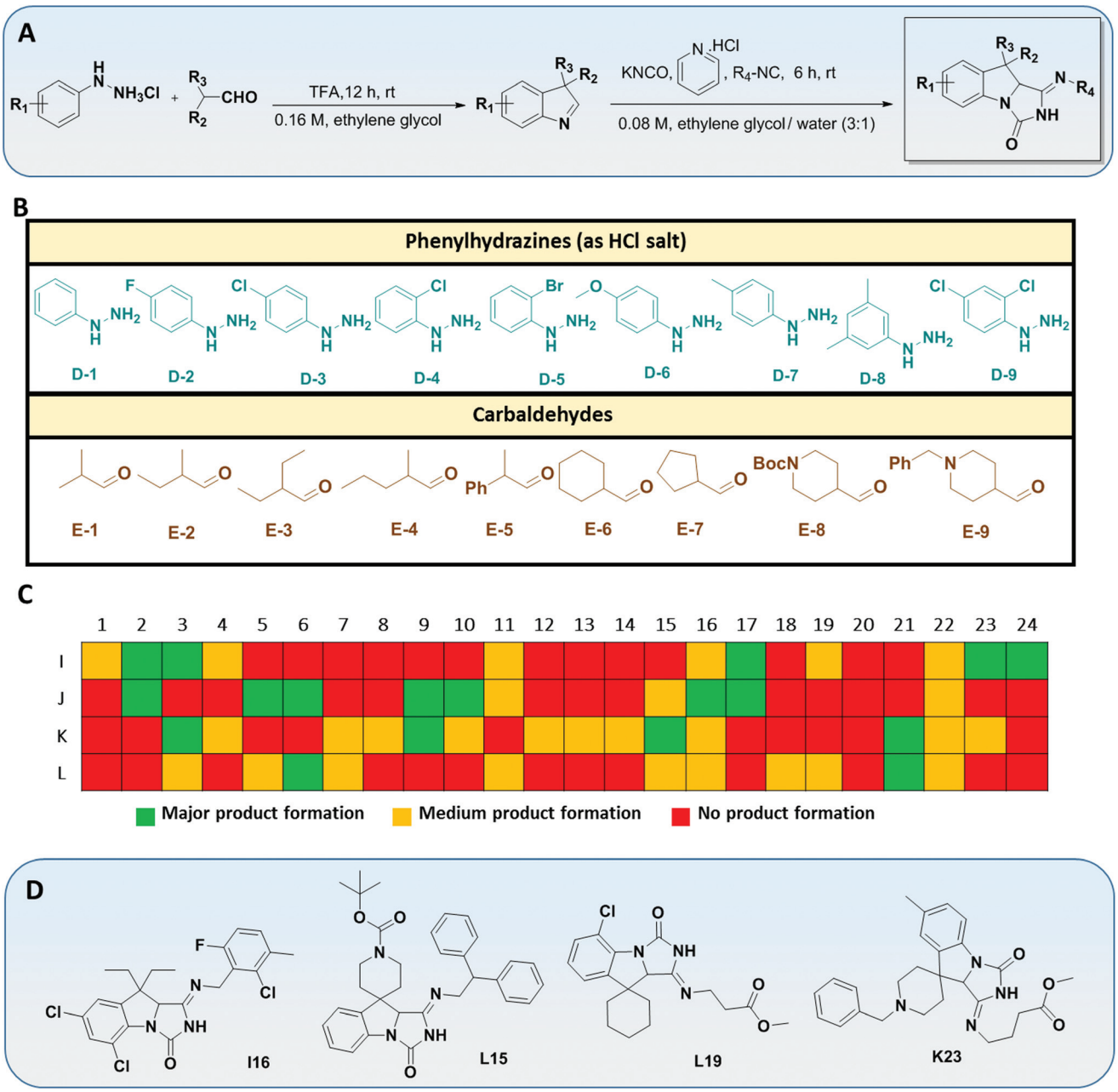

Fig. 5 Sequence of 2 reactions on a nanoscale in one pot. (A): *In situ* interrupted Fischer indole followed by Ugi hydantoin reaction. (B): Used phenyl hydrazine and aldehyde building blocks. (C): Quality control heat map based on SFC-MS data (ESI†). (D): Exemplary structures of formed compounds.

that the reduced analytical characterization (MS instead of NMR and IR) of nmol over mmol or higher scale reactions is a clear trade-off of the herein proposed miniaturization and acceleration of synthetic chemistry and might lead in a few cases to misassignment of the structure.

High throughput screening (HTS) is a mainstay to the current drug discovery paradigm. Million-sized compound collections of small molecules each on a mg scale are housed in the libraries of pharmaceutical companies and form the basis of the HTS. Renewal of the content of the compound libraries is a very resource and time-demanding process. ADE-enabled chemistry could be advantageously used to pre-screen the feasibility of the mg-scale synthesis of a large number of building block combinations including unusual and expensive reagents. In traditional mmol-scale chemistry, this would be impractical or impossible due to resource, time and cost constraints.

Further potential applications of this technology include high throughput synthesis and *in situ* screening for protein target binding. The feasibility and advantage of miniaturized synthesis and at the same time the successful screening of unpurified reaction mixtures have already been established.[38]

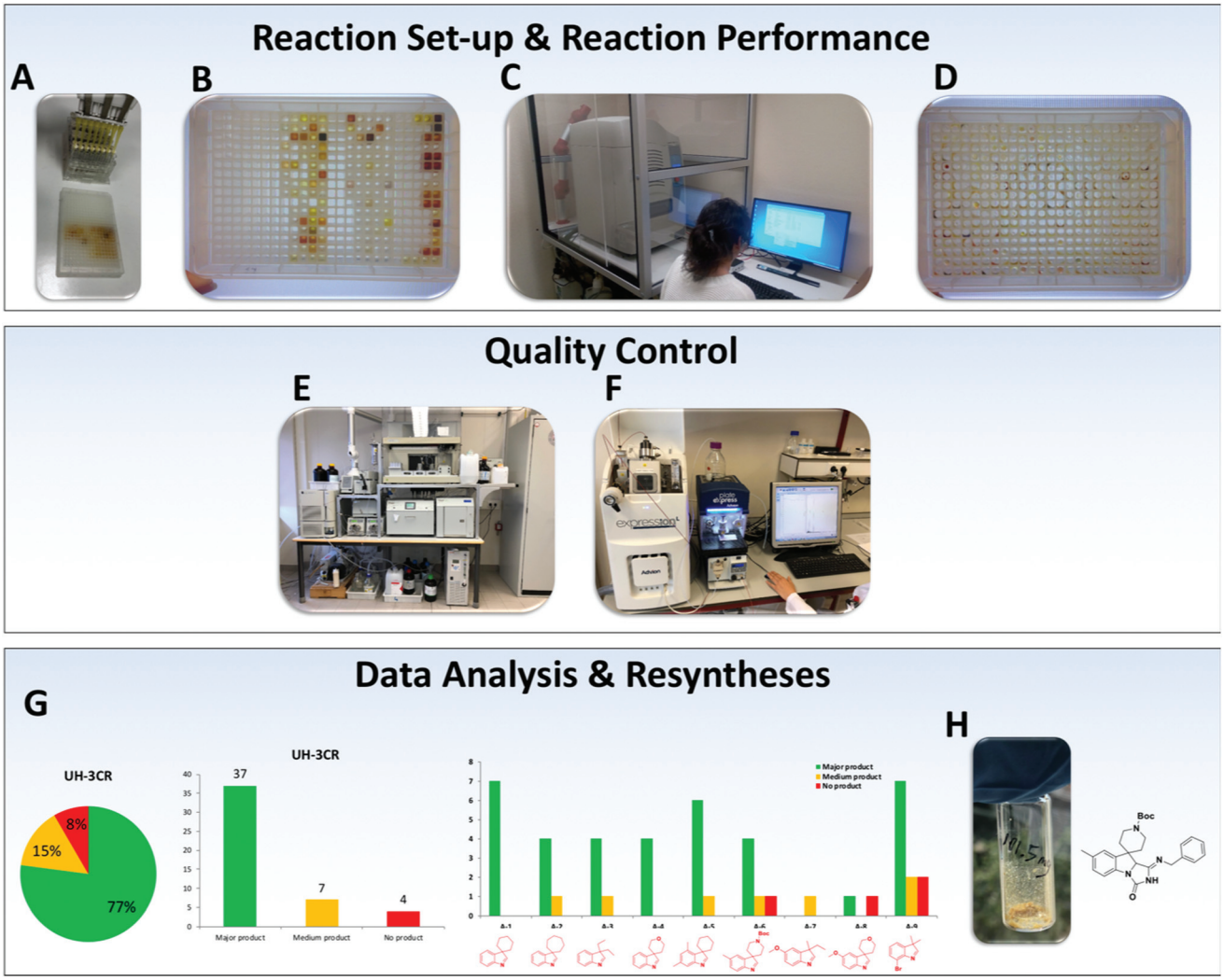

Fig. 6 Workflow of automated and accelerated ADE-enabled syntheses. Above: Preparation of stock solutions of building blocks (A) and transfer into 386-well source plates (B); ADE workplace with an ECHO555 in a chemical hood and an external remote computer control (C); a 384-well destination plate (D). Middle: Quality control with SFC-MS (E) and TLC-UV-MS (F). Bottom: Data analysis (G) and resynthesis of compounds on a 0.5 mmol scale (H).

Thus, it is conceivable that ADE-enabled organic high throughput synthesis can be synergistically combined with miniaturized and fast ligand–receptor or even phenotypical screening.

Conflicts of interest

There are no conflicts to declare.

Acknowledgements

We thank Pravin Patil, Konstantinos Neochoritis, Dominik Zahr, Joe Olechno, Richard Elson and Tryfonas Zarganis for helpful discussions and Nicolo Tito for writing an extension of the RandReact program. This project has received funding (to A. D.) from the European Lead Factory (IMI) under grant agreement number 115489, the Qatar National Research Foundation (NPRP6-065-3-012), the European Union's Horizon 2020 research and innovation programma under the Marie Sklodowska-Curie (ITN "Accelerated Early stage drug dIScovery", grant agreement no 675555; Cofunds ALERT, (grant agreement no 665250) and PROMINENT (grant agreement no 754425)). S. S. was supported by a postdoctoral research fellowship from Kankerbestrijding (KWF grant agreement no 10504). R. X. and L. G. were supported by Chinese Scholarship Council grants. M. A. M. was supported by a NIH grant (2R01GM097082-05).

References

1 A future that works: automation, employment, and productivity, https://www.mckinsey.com/~/media/mckinsey/fea-

tured20insights/Digital20Disruption/Harnessing20automation20for20a20future20that20works/MGI-A-future-that-works-In-brief.ashx.
2 J. Zhou, P. Li, Y. Zhou, B. Wang, J. Zang and L. Meng, *Engineering*, 2018, **4**, 11–20.
3 R. Y. Zhong, X. Xu, E. Klotz and S. T. Newman, *Engineering*, 2017, **3**, 616–630.
4 N. Hata, P. Moreira and G. Fischer, *TMRI*, 2018, **27**, 19–23.
5 K. C. Nicolaou, *Proc. R. Soc. A*, 2014, **470**, 20130690.
6 A. Kreimeyer, P. Eckes, C. Fischer, H. Lauke and P. Schuhmacher, *Angew. Chem., Int. Ed.*, 2015, **54**, 3178–3195.
7 M. Whitesides George, *Angew. Chem., Int. Ed.*, 2015, **54**, 3196–3209.
8 G. Prieto and F. Schüth, *Angew. Chem., Int. Ed.*, 2015, **54**, 3222–3239.
9 R. B. Merrifield, J. M. Stewart and N. Jernberg, *Anal. Chem.*, 1966, **38**, 1905–1914.
10 M. Panza, S. G. Pistorio, K. J. Stine and A. V. Demchenko, *Chem. Rev.*, 2018, **118**(17), 8105–8150.
11 M. Trobe and M. D. Burke, *Angew. Chem., Int. Ed.*, 2018, **57**, 4192–4214.
12 S. Ota, H. Kitagawa and S. Takeuchi, *Anal. Chem.*, 2012, **84**, 6346–6350.
13 M. Srisa-Art, A. J. deMello and J. B. Edel, *Anal. Chem.*, 2007, **79**, 6682–6689.
14 P. Anzenbacher Jr. and M. A. Palacios, *Nat. Chem.*, 2009, **1**, 80–86.
15 R. Ellson, *Drug Discovery Today*, 2002, **7**, S32–S34.
16 S. Malaquin, M. Jida, J.-C. Gesquiere, R. Deprez-Poulain, B. Deprez and G. Laconde, *Tetrahedron Lett.*, 2010, **51**, 2983–2985.
17 A. Váradi, T. C. Palmer, N. Haselton, D. Afonin, J. J. Subrath, V. Le Rouzic, A. Hunkele, G. W. Pasternak, G. F. Marrone, A. Borics and S. Majumdar, *ACS Chem. Neurosci.*, 2015, **6**, 1570–1577.
18 H. Wehlan, J. Oehme, A. Schäfer and K. Rossen, *Org. Process Res. Dev.*, 2015, **19**, 1980–1986.
19 Y. Huang and A. Dömling, *Mol. Diversity*, 2011, **15**, 3–33.
20 J. M. Saya, R. Berabez, P. Broersen, I. Schuringa, A. Kruithof, R. V. A. Orru and E. Ruijter, *Org. Lett.*, 2018, **20**, 3988–3991.
21 C. Kalinski, H. Lemoine, J. Schmidt, C. Burdack, J. Kolb, M. Umkehrer and G. Ross, *Synthesis*, 2008, 4007–4011.
22 A. Znabet, M. M. Polak, E. Janssen, F. J. J. de Kanter, N. J. Turner, R. V. A. Orru and E. Ruijter, *Chem. Commun.*, 2010, **46**, 7918–7920.
23 A. D. Borthwick, J. Liddle, D. E. Davies, A. M. Exall, C. Hamlett, D. M. Hickey, A. M. Mason, I. E. D. Smith, F. Nerozzi, S. Peace, D. Pollard, S. L. Sollis, M. J. Allen, P. M. Woollard, M. A. Pullen, T. D. Westfall and D. J. Stanislaus, *J. Med. Chem.*, 2012, **55**, 783–796.
24 J. Popovici-Muller, R. M. Lemieux, E. Artin, J. O. Saunders, F. G. Salituro, J. Travins, G. Cianchetta, Z. Cai, D. Zhou, D. Cui, P. Chen, K. Straley, E. Tobin, F. Wang, M. D. David, V. Penard-Lacronique, C. Quivoron, V. Saada, S. de Botton, S. Gross, L. Dang, H. Yang, L. Utley, Y. Chen, H. Kim, S. Jin, Z. Gu, G. Yao, Z. Luo, X. Lv, C. Fang, L. Yan, A. Olaharski, L. Silverman, S. Biller, S.-S. M. Su and K. Yen, *ACS Med. Chem. Lett.*, 2018, **9**, 300–305.
25 D. J. Foley, A. Nelson and S. P. Marsden, *Angew. Chem., Int. Ed.*, 2016, **55**, 13650–13657.
26 S. W. Krska, D. A. DiRocco, S. D. Dreher and M. Shevlin, *Acc. Chem. Res.*, 2017, **50**, 2976–2985.
27 R. C. Cioc, E. Ruijter and R. V. A. Orru, *Green Chem.*, 2014, **16**, 2958–2975.
28 E. Ruijter, R. Scheffelaar and V. A. Orru Romano, *Angew. Chem., Int. Ed.*, 2011, **50**, 6234–6246.
29 K. G. Liu and A. J. Robichaud, *Tetrahedron Lett.*, 2007, **48**, 461–463.
30 Y.-D. Shao and S.-K. Tian, *Chem. Commun.*, 2012, **48**, 4899–4901.
31 V. Estévez, L. Kloeters, N. Kwietniewska, E. Vicente-García, E. Ruijter and R. V. A. Orru, *Synlett*, 2017, **28**, 376–380.
32 P. M. Collins, J. T. Ng, R. Talon, K. Nekrosiute, T. Krojer, A. Douangamath, J. Brandao-Neto, N. Wright, N. M. Pearce and F. von Delft, *Acta Crystallogr.*, 2017, 246–255, DOI: 10.1101/085712.
33 A. Buitrago Santanilla, E. L. Regalado, T. Pereira, M. Shevlin, K. Bateman, L.-C. Campeau, J. Schneeweis, S. Berritt, Z.-C. Shi, P. Nantermet, Y. Liu, R. Helmy, C. J. Welch, P. Vachal, I. W. Davies, T. Cernak and S. D. Dreher, *Science*, 2015, **347**, 49–53.
34 S. Lin, S. Dikler, W. D. Blincoe, R. D. Ferguson, R. P. Sheridan, Z. Peng, D. V. Conway, K. Zawatzky, H. Wang, T. Cernak, I. W. Davies, D. A. DiRocco, H. Sheng, C. J. Welch and S. D. Dreher, *Science*, 2018, **6402**, eaar6236.
35 T. Cernak, N. J. Gesmundo, K. Dykstra, Y. Yu, Z. Wu, Z.-C. Shi, P. Vachal, D. Sperbeck, S. He, B. A. Murphy, L. Sonatore, S. Williams, M. Madeira, A. Verras, M. Reiter, C. H. Lee, J. Cuff, E. C. Sherer, J. Kuethe, S. Goble, N. Perrotto, S. Pinto, D.-M. Shen, R. Nargund, J. Balkovec, R. J. DeVita and S. D. Dreher, *J. Med. Chem.*, 2017, **60**, 3594–3605.
36 K. D. Collins, T. Gensch and F. Glorius, *Nat. Chem.*, 2014, **6**, 859–871.
37 M. Shevlin, *ACS Med. Chem. Lett.*, 2017, **8**, 601–607.
38 N. J. Gesmundo, B. Sauvagnat, P. J. Curran, M. P. Richards, C. L. Andrews, P. J. Dandliker and T. Cernak, *Nature*, 2018, **557**, 228–232.

